Theor Chem Account (2008) 119:343–354
DOI 10.1007/s00214-007-0392-5

REGULAR ARTICLE

Structural and vibrational theoretical analysis of protonated formaldehyde in its $\tilde{X}^1A'$ ground electronic state

María Eugenia Castro · Alfonso Niño · Camelia Muñoz-Caro

Received: 27 July 2007 / Accepted: 13 September 2007 / Published online: 10 October 2007

Abstract A structural and vibrational study of protonated formaldehyde (H_2COH^+) in its ground electronic state, at the CCSD/cc-pVTZ theory level, is presented. The variation of the molecular structure with the torsion angle shows clear dependence of the H_2C wagging and COH angles. Anharmonic one- and two-dimensional vibrational models for two out-of-plane vibrational modes (H_2C torsion, and H_2C wagging) are constructed. Since H_2COH^+ is classified under a G_4 non-rigid group, the vibrational Hamiltonians are factorized using the symmetry of the G_4 group and solved variationally. The one-dimensional results for torsion and wagging yield fundamental frequencies are 844.12 and 1,252.89 cm^{-1}, respectively. A two-dimensional COH angle + torsion model gives a torsion frequency of 762.32 cm^{-1}. Finally, a wagging + torsion model predicts frequencies of 931.93 and 1,255.82 cm^{-1} for torsion and wagging, respectively. The variation of frequency values for torsion suggests an important coupling between this mode and the bending and wagging vibration modes.

Keywords Anharmonic model · Structural study · Torsion · Wagging · Energy vibrational levels · Protonated formaldehyde

1 Introduction

Protonated formaldehyde plays important roles in a wide variety of processes, such as the combustion of hydrocarbon fuels, atmospheric pollution chemistry, chemistry on surfaces, catalytic processes, hydrogenation/dehydrogenation chemistry, and especially in the chemistry governing molecular formation in interstellar medium. Most theoretical models about formation and evolution of molecules in interstellar clouds predict that protonated formaldehyde, H_2COH^+, plays an important role in the formation and depletion of formaldehyde through ion–molecule reactions in gas phase and surface reactions on dust grains [1–3].

Measurements of heats of formation showed that the most stable isomer of H_2COH^+ bears the additional proton on the oxygen atom [4]. Early theoretical studies using ab initio methodology [5–9] also arrived at the same conclusion. The first spectroscopic identification of protonated formaldehyde in the laboratory was carried out by Amano and Warner in 1989 [3] using infrared spectroscopy. These authors found a frequency of 3,422.8 cm^{-1} for the fundamental band of the O–H stretching mode. DeFrees and McLean [10] obtained values of 3,457 and 3,531 cm^{-1} for this mode using ab initio calculations at the HF/6-31G(d) and MP2/6-31G(d) levels, respectively.

Starting from the IR spectroscopy measurements of Amano and Warner [3], Chomiak et al. [11] obtained more accurate rotational transition frequencies using microwave spectroscopy, in order to identify protonated formaldehyde in the interstellar media. Using this information, H_2COH^+ was detected in several high-mass star-forming regions by Ohishi et al. in 1996 [12]. These authors assigned unmixed bands of microwave spectrum transitions, indicating that H_2COH^+ exists in cold and dark clouds.

Several theoretical works have been carried out on protonated formaldehyde [5–10,13–32]. All these studies show a planar structure of C_s symmetry as the minimum energy structure, in agreement with the experimental data. Harmonic frequencies have been computed in several of these works

M. E. Castro · A. Niño · C. Muñoz-Caro (✉)
Grupo de Química Computacional y Computación de Alto Rendimiento, Escuela Superior de Informática,
Universidad de Castilla-La Mancha, Paseo de la Universidad 4,
13071 Ciudad Real, Spain
e-mail: camelia.munoz@uclm.es

[10,17,20,21,23,24,26,28] for the equilibrium geometry. The values have been contrasted with the available experimental data for the O–H stretch mode in the cationic form of protonated formaldehyde [3], and with some vibrational modes of the $\tilde{B}^2A'(3p)$ radical [23,33,34]. The considered vibration modes have been the H_2C scissors and the out-of-phase HCOH bending [33,34], as well as the in-phase HCOH bending, CO stretching [23,33,34], and OH^+ torsion [23]. In most cases, the theoretical values were in good agreement with the experimental data.

Most theoretical works focussed on the energy variation for the OH (H_2C) moiety rotation around the C-O bond [5,13,14,16,19,22,23]. In this form, different values for the torsion barrier have been found. Thus, a value of 10,982.31 cm^{-1} was found by Ros [5] in a LCAO HF MO SCF approximation. More recent ab initio studies have reported barrier values of 9,093.6 and 8,464.1 cm^{-1} at the MP3/6-31G(d) and MP3/3-21G levels [19], respectively. The saddle point considered in these studies corresponds to a rotated structure with a torsion angle of 90°. In the last work [19], the saddle point geometry was allowed to relax fully. In a more recent MP2/6-311G(2df,2p) study by Johnson and Hudgens [23], a barrier of 8,331 cm^{-1} was found.

The total energy variation of H_2COH^+ as a function of the COH valence angle has also been considered [5,13,14,16,22,25]. Due to the symmetry of the molecule, the COH angle is symmetric with respect to the structure with collinear C, O, and H atoms. Thus, it is possible to speak about a bending barrier. The bending barrier has been calculated by several authors. Thus, Ros [5] found a 6,015.79 cm^{-1} value using a LCAO HF MO SCF approximation. Ab initio computations provided values of 8,499.05 and 8,324.17 cm^{-1}, from calculations at the MP2(FC)/6-311+G(d,p) and QCISD(T) (FC)/6-311+G(3df,2p)//MP2(FC)/6-311+G(d,p) levels, respectively [25]. These values correspond to a maximum, for the bending motion, in a structure of C_{2v} symmetry with a COH valence angle of 180°.

The torsion motion of the proton in H_2COH^+ (or more correctly, the torsion of the H_2C moiety) can be considered a periodic motion, with an angular dependence satisfying the boundary conditions of a free rotor. Torsion and bending motions have been considered as the mechanisms for the transformation between the two equivalent C_s planar structures of the molecule. In an early study, Ros [5] found more energetically favourable the motion in the plane (bending) than the torsional motion. Purcell and Collins [13] suggested that the motion of the COH angle towards a linear structure has associated a fair amount of mechanical anharmonicity. Ohkubo et al. [14] and Bhattacharyya et al. [16] considered the pure rotational and bending motions as the most important transformation processes in H_2COH^+. Subsequently, ab initio studies [22,25] were carried out on both motions. Stern et al. [22] suggested that the planar pathway was energetically preferred to the torsional pathway in protonated formaldehyde. These authors obtained a bending barrier smaller than the torsional barrier at the HF/4-31G level. Suarez and Sordo [25] characterized the saddle point structure for the bending motion as a C_{2v} structure at the MP2/6-311G+(d,p) theory level. In this form, the work above mentioned reported two different values of energy barriers, one for the motion of the COH angle and other one for the OH torsion in the molecule.

On the other hand, up to now, only one study has been reported considering anharmonic models, in particular for the two out-of-plane modes in H_2COH^+: torsion and wagging [23]. This work computes the vibrational energy levels of the coupled modes using the grid Fourier Hamiltonian [35], estimating the reduced inertia moments for the torsion and wagging motions. The authors conclude that the torsion and H_2C wagging motions are mixed modes. The study suggests that the cation exhibits weak vibrational couplings for the spectroscopically important vibrational levels, unlike the radical, where both motions are strongly coupled for all the vibrational levels. This study predicts that mode mixing in the cation becomes strong as the high torsion barrier is approached.

In this work, we present a theoretical study of protonated formaldehyde as a function of the OH torsional, and H_2C wagging motions, also considering the effect of the COH bending angle. The coupling between these coordinates is explicitly taken into account. One-dimensional potential energy surfaces are determined for torsion and wagging. Two-dimensional bending + torsion and wagging + torsion motions are also considered. In this form, energy barriers and saddle points are obtained, and the mechanism of interconversion between the two symmetry equivalent C_s structures is fully characterized. Anharmonic vibrational models are constructed, and solved variationally. The Hamiltonian is simplified and the energy levels are classified by using the non-rigid symmetry group of the molecule. In this form, new values are predicted for the torsional and wagging vibrational frequencies.

2 Methodology

The numbering convention used in this work for protonated formaldehyde is shown in Fig. 1a. Using this convention, the most direct definition of the torsional coordinate for the OH (H_2C) group, θ, is the dihedral H3C2O1H5, see Fig. 1b. The bending motion is described by α that corresponds to the C2O1H5 angle, see Fig. 1a. When the H_2C wagging mode is taken into account, the θ torsion angle and τ wagging coordinates are defined with the help of the dummy atom X shown in Fig. 1a. The τ coordinate is now defined as the H3C2XO1 dihedral, see Fig. 1c. In turn, the torsion coordinate is defined by the XC2O1H5 angle, see Fig. 1d.

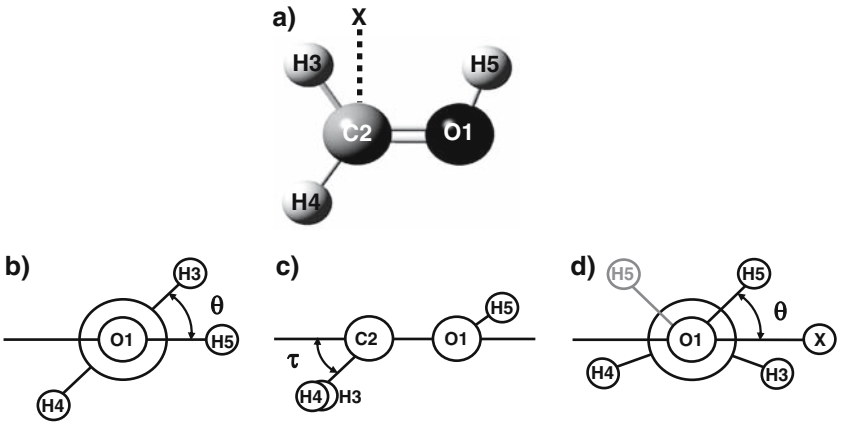

Fig. 1 **a** Structure and numbering convention of protonated formaldehyde. X denotes a dummy atom. **b** Newman projection showing the simplest definition of the θ angle. In this case the interchange of H3 and H4 is defined by the transformation $\theta \rightarrow \theta + 180°$. **c** Newman projection showing the τ wagging angle, defined as the dihedral between planes H3C2H4 and XC2O1. **d** Newman projection showing the θ torsional angle, defined respect to an arbitrary plane containing O1, C2 and the X dummy atom, for a conformation with a wagging angle $\tau \neq 0°$. In this case the interchange of H3 and H4 is defined by the transformation $\theta \rightarrow 180° - \theta$, see the grey image of H5

Different conformational analyses are performed computing different grids of points on the θ, α, and τ coordinates using ab initio methodology. In these calculations, correlation energy is accounted for at the CCSD level [36]. As basis set, we use the correlation consistent triple-zeta cc-pVTZ basis set [37]. The computations are carried out by fixing at each point the angles of interest, allowing the rest of the structure to relax fully. Stationary points, minima and saddle points are specifically located on the potential energy hypersurface. At each point of the different conformational analysis, harmonic frequencies are computed. In this form, in the different anharmonic vibrational models presented, we can account for the average effect of the remaining vibrations. Assuming a harmonic behaviour, this effect is obtained by including at each point of the potential energy hypersurface the contribution to the zero point energy of the vibrations not included in the vibrational model considered. This correction represents a Vibrational Adiabatic Correction, VAC. All the calculations are carried out with the Gaussian03 package [38], running on a Computational Grid formed by three clusters. Two of them (Ciudad Real, Spain) consist of 12 PCs each (Pentium IV, 2.4–3.0 GHz, 1 GB RAM). The third cluster (Puebla, Mexico) is formed by nine PCs (64-bit Opteron biprocessors, 1.66 GHz, 1 GB RAM). The Grid uses GridWay[1] as metascheduler, with Globus 4.0.3[2] as the basic Middleware. The three clusters run under the cluster configuration and management system Rocks.[3]

Protonated formaldehyde can be classified under a G_4 non-rigid group. This group is isomorphic to the C_{2v} point group and accounts for the interchange of the H3 and H4 atoms, (34) operation, see Fig. 1a, and the inversion of the electronic and nuclear coordinates, E* operation. The character table is shown in Table 1. When wagging is not taken into account, Fig. 1b shows that the effect of the (34) operation is to transform θ into $180 + \theta$. When wagging is considered, Fig. 1d shows that now the effect of (34) is to transform θ into $180 - \theta$.

Table 1 Character table for the G_4 permutation-inversion group of protonated formaldehyde

G_4	E	(34)	E*	(34)*
a_1	1	1	1	1
a_2	1	1	−1	−1
b_1	1	−1	−1	1
b_2	1	−1	1	−1

The anharmonic vibrational models considered in this work are derived from the general vibrational Hamiltonian [39–41]:

$$\hat{\mathrm{H}} = -\frac{\hbar^2}{2} \sum_{i=4}^{3N-3} \sum_{j=4}^{3N-3} \left[g_{ij} \frac{\partial^2}{\partial q_i \partial q_j} + \left(\frac{\partial g_{ij}}{\partial q_i} \right) \frac{\partial}{\partial q_j} \right] + V(q_1, \ldots, q_{N-6}) \quad (1)$$

where the q_is represent vibrational coordinates, g_{ij} are the elements of the roto-vibrational G matrix, and V is the potential function, which depends on the q_is coordinates. In turn, the roto-vibrational G matrix is defined as [41]

$$G = \begin{pmatrix} I & X \\ X^T & Y \end{pmatrix}^{-1} \quad (2)$$

[1] www.gridway.org, last visit on 5 September 2007

[2] www.globus.org, last visit on 5 September 2007

[3] www.rocksclusters.org, last visit on 5 September 2007

Table 2 Structural parameters of protonated formaldehyde in its planar, C_s, equilibrium structure. The numbering convention is shown in Fig. 1. Distances in Angstroms and angles in degrees

Parameter	Value[a]	Value[b]	Value[c]	Value[d]	Value[e]	Value[f]	Value[g]
C2O1	1.246	1.246	1.251	1.249	1.259	1.369	1.248
H5O1	0.978	0.980	0.979	0.982	0.992	0.963	0.980
H3C2	1.088	1.086	1.093	1.089	1.090	1.082	1.074
H4C2	1.086	1.084	1.091	1.091	1.090	1.078	1.104
∠H3C2O1	121.6	121.6	121.7	121.7	115.4	118.3	–
∠H5O1C2 (α)	115.1	115.1	114.5	114.2	–	–	115.5
∠H4C2O1	115.9	115.7	–	–	115.3	113.0	122.0

[a] This work, data at the CCSD/cc-pVTZ level
[b] Ref. [23], data at the MP2/6-311(2df, 2p) level
[c] Ref. [25], data at the QCISD(FC)/6-311+G(d, p) level
[d] Ref. [25], data at the MP2(FC)/6-311+G(d, p) level
[e] Ref. [29], data at the QCISD/6-31G(d) level
[f] Ref. [29], data at the MP2/6-311+G(2d, p) level
[g] Ref. [32], data at the MR-CISD+Q level

Here, I represents the inertia tensor, i.e. the overall rotation contribution, Y corresponds to the pure vibration contribution, and X represents the vibration–rotation interaction (Coriolis term). The elements of I, X and Y are obtained from the molecular structure as,

$$
\begin{aligned}
I_{ii} &= \sum_{\alpha}^{n} m_\alpha \left[(r_\alpha)^2 - (r_{\alpha i})^2 \right] \\
I_{ij} &= -\sum_{\alpha}^{n} m_\alpha r_{\alpha i} r_{\alpha j} \\
X_{ij} &= \sum_{\alpha}^{n} m_\alpha \left[r_\alpha \left(\frac{\partial r_\alpha}{\partial q_i} \right)^2 \right]_j \\
Y_{ij} &= \sum_{\alpha}^{n} m_\alpha \left(\frac{\partial r_\alpha}{\partial q_i} \right) \left(\frac{\partial r_\alpha}{\partial q_j} \right)
\end{aligned}
\tag{3}
$$

where the α index runs on the atoms in the molecule. All the calculations related to the G matrix are carried out with the KICO program [42]. For the different anharmonic vibrational models build in this work, the kinetic and potential functions are expressed as Fourier or Taylor expansions of symmetry adapted to the a_1 representation of the G_4 non-rigid group of protonated formaldehyde [43–45].

The vibrational Hamiltonian shown in Eq. (1) is variationally solved using the general formalism described in Ref. [43]. In the present work, we use real free rotor basis functions for torsion, and harmonic oscillator basis functions for bending and wagging. As basis set we use symmetry adapted basis functions obtained by projecting on the irreducible representations of the G_4 group. In this form, the Hamiltonian matrix is factorized in blocks, and the energy levels are automatically classified by symmetry. In the Hamiltonian matrix, the integrals involving free rotor or harmonic oscillator wavefunctions are computed as described in references [44] and [45]. All the vibrational calculations are carried out with the LAVCA program [46].

3 Results and discussion

After full molecular relaxation, the most stable structure is found planar, $\theta = 0°$, with a C2O1H5 bending angle (α) of 115.12°, and a H3C2O1H4 dihedral of 180°, (See Fig. 1). This structure has C_s symmetry, in agreement with the geometries reported in previous theoretical work [5–9,15, 17–20,22–25,27–32]. The optimized structural parameters are collected in Table 2 where they are compared with some previous results.

To analyse the variation of the structure as a function of the torsion angle, we vary θ from 0° to 90° in increments of 10° (10 points). For each fixed θ value, the rest of the geometry is allowed to fully relax. Figure 2 shows the resulting potential energy curve as a function of the θ angle, with and without the VAC correction. The maximum of the curve corresponds to a structure of C_{2v} symmetry. This is a first-order saddle point on the full hypersurface located at $\theta = 90°$, with $\alpha = 180°$. Thus, the C2, O1 and H5 atoms are collinear. Therefore, strictly speaking, in this structure the θ angle is undefined. These results show that there is just one maximum defining the barrier for both, torsion and bending, in contrast with previous results reporting independent barriers [5,13,14,16,19,22,23,25]. Some authors [19] reported a fully relaxed structure with $\alpha \neq 180°$ for the torsion saddle point. The difference is due to the use in these previous works of a fixed C2O1H5 angle when considering the torsional motion [19].

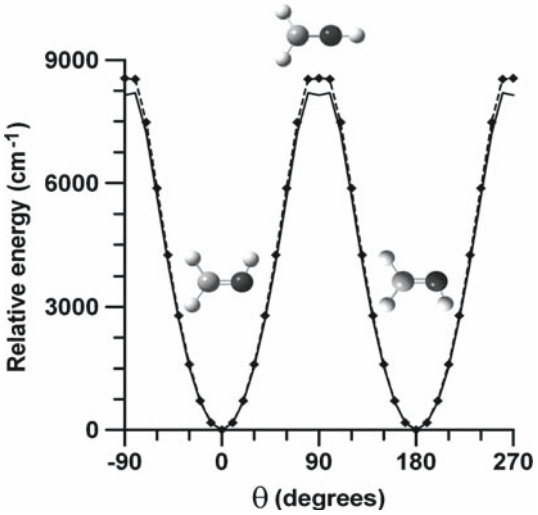

Fig. 2 Potential energy variation of protonated formaldehyde as a function of the θ torsional angle. The structures at the minima and maximum (saddle point, as described in the text) are included. *Diamonds* mark the data points computed at the CCSD/cc-pVTZ level. *Continuous line* corresponds to the VAC corrected data

Table 3 Barriers for torsion and bending for protonated formaldehyde. Energy data in cm^{-1}

Calculation level	Torsion barrier	Bending barrier
CCSD/cc-pVTZ[a]	8,550.95	8,550.95
LCAO HF MO SCF[b]	10,982.31	6,015.79
CNDO/2[c]	7,694.61	8,044.37
INDO-SCF[d]	8,051.36	4,963.03
MP3/6-31G(d)[e]	9,093.60	–
MP3/3-21G[e]	8,464.10	–
HF/STO-4G[f]	8,638.90	4,511.80
MP2/6-311G(2df, 2p)[g]	8,331.00	–
MP2(FC)/6-311+G(d,p)[h] QCISD(T)(FC)/6-311+G//	–	8,499.05
MP2(FC)76-311+G(d,p)[h]	–	8,324.17

[a] This work, data at the CCSD/cc-pVTZ theory level
[b] Ref. [5]
[c] Ref. [13]
[d] Ref. [14]
[e] Ref. [19]
[f] Ref. [22]
[g] Ref. [23]
[h] Ref. [25]

The present calculations yield a torsion barrier of 8,550.95 cm^{-1}. This value is in the order of previous theoretical values, as shown in Table 3. In particular, the present value is close to the 8,331 cm^{-1} reported by Johnson and Hudgens [23], from a two-dimensional potential energy surface for wagging + torsion, obtained at the MP2/6-311G (2df, 2p) level. Inclusion of the average effect of the remaining vibrations in the torsion, VAC, reduces the torsion barrier to 8,145.19 cm^{-1}, (see Fig. 2).

The variation of the molecular structure with torsion is illustrated in Fig. 3, using the α bending and the H4C2O1H3 dihedral (related to the H_2C wagging) angles (see Fig. 1). We observe that α increases with θ, reaching a maximum of 180°. On the other hand, the H4C2O1H3 dihedral distorts from its original 180° value for $\theta = 0°$ to 158.4° for $\theta = 60°$. A planar structure is recovered for $\theta = 90°$. Therefore, maximum deviations from equilibrium of 64.87° and −21.60° are observed for the θ and H4C2O1H3 angles, respectively. The slope of the curve in Fig. 3a shows a small variation of α with θ in the zone of not very large energy values (a maximum of about 4,000 cm^{-1}, i.e. a range of θ about ±60°, see Fig. 1). On the other hand, Fig. 3b shows a larger variation of dihedral H4C2O1H3 in the same zone. However, for θ values larger than 60°, the variation of α follows an increasing trend, whereas τ decreases to its original value. Since θ is associated to the torsion, α to the bending, and dihedral H4C2O1H3 to the wagging vibration modes, the present results suggest that the torsional and bending motions are as coupled as torsion and wagging, both out-of-plane motions. With respect to the C2O1 bond, the equilibrium value is 1.246 Å. The value increases upon rotation, reaching 1.253 Å for $\theta = 60°$, and decreasing to a minimum of 1.222 Å for $\theta = 90°$. The O1H5 bond distance shows a similar variation. We find an equilibrium value of 0.978 Å. The distance increases to 0.979 Å for $\theta = 50°$, and decreases to a minimum of 0.966 Å for $\theta = 90°$. Those changes can be attributed to the unfavourable orientation of the out-of-plane O1 $2p_z$ orbital for conjugation with the C2 $2p_z$ orbital, upon rotation until θ reaches about 60°. From there, the orientation is more and more favourable when θ approaches 90° and the C2, O1 and H3 atoms are collinear.

Harmonic frequencies are compared in Table 4 to previous harmonic theoretical and experimental data, using the notation of Johnson and Hudgens [23]. In this notation, the lowest frequency vibrations corresponding to the bending, torsion and wagging motions, are identified as ν_7, ν_8, and ν_9, respectively. The harmonic frequency for torsion calculated in our work is $\nu_8 = 1{,}042.44\ cm^{-1}$. This value agrees with the 1,034 cm^{-1} computed at the CCSD/aug-cc-pVDZ level by Del Bene et al. [26], and the 1,052 cm^{-1} of Blowers and Masel [29], obtained at the MP2/6-311+G(2d,p) level, see Table 4. However, our value is larger than the experimental value of 993 cm^{-1} for the protonated formaldehyde $\tilde{B}^2A'(3p)$ radical reported by Johnson and Hudgens [23], and taken by these authors as an estimation for the torsional frequency of the cation. On the other hand, the fundamental frequency for the ν_7 bending mode is found 1,129.49 cm^{-1}. This value is in good agreement with previous values reported

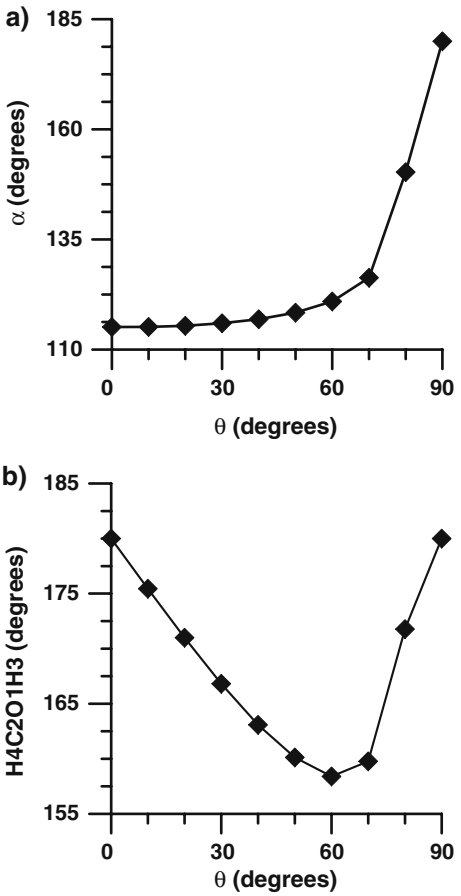

Fig. 3 Variation of the molecular structure of protonated formaldehyde with torsion. **a** α bending angle. **b** H4C2O1H3 dihedral angle

in the literature, such as the $1{,}135\,\mathrm{cm}^{-1}$ obtained at the MP2//HF/6-31G(d,p) theory level [28] and the $1{,}129\,\mathrm{cm}^{-1}$ [29] obtained at the MP2/6-311+G(2d,p) level, see Table 4. The fundamental frequency for this mode is close to the experimental value of $1{,}107\,\mathrm{cm}^{-1}$ for the $\tilde{B}^2A'(3p)$ radical [34]. Finally, the ν_9 wagging mode is found $1{,}266.96\,\mathrm{cm}^{-1}$, in agreement with the $1{,}275\,\mathrm{cm}^{-1}$ and $1{,}250\,\mathrm{cm}^{-1}$ obtained at the MP2//HF/6-31G(d,p) and MP2/6-311+G(2d,p) theory levels as references [28] and [29], respectively, see Table 4. Our present value is 7.8% larger than the $1{,}175\,\mathrm{cm}^{-1}$ reported by Johnson and Hudgens [23], from a two-dimensional wagging+torsion anharmonic model.

More accurate frequency estimations for the related ν_7, ν_8, and ν_9 modes could be obtained by building anharmonic vibrational models. An anharmonic model for torsion can be readily constructed to obtain torsional vibrational energy levels. As torsional coordinate we use the θ angle, which is the same torsional coordinate used in the work of Johnson and Hudgens [23]. The kinetic values, B_θ, are obtained from the roto-vibrational G matrix at each point of the conformational analysis. In particular, for the equilibrium conformation B_θ is found to be $33.09\,\mathrm{cm}^{-1}$. Kinetic and potential functions are obtained by fitting these data to Fourier series of symmetry adapted to the a_1 representation of the G_4 non-rigid group. The potential energy function includes at each point the average effect of the remaining vibrations (i.e., the vibrational adiabatic correction, VAC, obtained as the ZPE contribution of these vibrations). The B_θ value is undefined for the $\theta = 90°$ conformation, as a consequence of the collinearity of the C2, O1, and H5 atoms. However, due to the very high value of the energy barrier, the probability to find the system for θ values close to 90° is negligible [47]. Thus, in the fit of the kinetic term, we have considered B_θ values in the range $\theta = 0°–70°$. This range was selected as the one giving the best regression equation according to the R^2 (quadratic correlation coefficient) and σ (standard deviation) parameters. This interval corresponds to a potential energy variation from 0.00 to $7{,}478.99\,\mathrm{cm}^{-1}$, see Fig. 2. The resulting fitted expressions are collected in Table 5. For the potential, we obtain a good correlation, with $R^2 = 0.999$. On the other hand, σ is found $105.83\,\mathrm{cm}^{-1}$. This value corresponds to a small deviation since, in relative terms, the variation of the predicted with respect to the observed values is small. The apparent large σ value arises from the absolute contribution of the data at high energy values.

The Hamiltonian is variationally solved using free rotor basis functions of symmetry adapted to the irreducible representations of the H_2COH^+ G_4 non-rigid group, (see Table 1). A total of 26 symmetry-adapted basis functions is used for the a_1 representation, and 25 for the a_2, b_1, and b_2 representations. The number of basis functions is selected as the minimum needed to attain convergence in the first ten energy levels for each irreducible representation. The torsional energy levels are collected in Table 6. We can observe that two states of different symmetry are found for each energy value. These two levels are due to the tunnelling splitting through the torsional barrier. This barrier is so high that both levels lie together. We find that the fundamental frequency for the eight normal mode, $\nu_8 = 0 \rightarrow 1$, is $844.12\,\mathrm{cm}^{-1}$. This value disagrees with the $978\,\mathrm{cm}^{-1}$ estimated by Johnson and Hudgens [23], from a wagging + torsion two-dimensional calculation. The main difference between the model of Johnson and Hudgens [23] and ours is in the kinetic part of the vibrational Hamiltonian. These authors use a fixed geometry corresponding to the structure of a radical H_2COH^+. In this case, by population of an antibonding orbital of π symmetry, the structure pyramidalizes due to the loss of sp^2 character of the carbon atom. A similar effect is found in acetaldehyde when going from the ground singlet state to the first excited singlet or triplet states [39,43,48–50]. However, as shown above, the structure of the protonated formaldehyde cation is planar. Thus, the use of a pyramidalized structure is translated in incorrect kinetic terms. In addition, in Ref. [23] kinetic terms are assumed independent of θ and are not obtained from the roto-vibrational G matrix.

Table 4 Calculated and experimental vibrational frequencies of protonated formaldehyde. Data in cm^{-1}. The normal modes notation is taken from Ref. [23], where the symmetry is referred to the C_s point group

Normal mode	Value[a]	Value[b]	Value[c]	Value[d]	Value[e]	Value[f]	Experimental values		
$\nu_1(a')$ OH stretch	3,656.97	3,511	3,625	3,635	3,386	3,594	3,422.8[g]		
$\nu_2(a')CH_2$ asym stretch	3,269.59	3,214	3,280	3,378	3,155	3,286			
$\nu_3(a')CH_2$ sym stretch	3,127.91	3,068	3,129	3,210	3,014	3,133			
$\nu_4(a')CH_2$ scissors	1,502.51	1,463	1,477	1,522	1,424	1,507	1,465[h]	1,459[i]	
$\nu_5(a')$ in phase HCOH bend	1,411.05	1,356	1,410	1,404	1,341	1,402	1,357[h]	1,351[i]	1,370[j]
$\nu_6(a')$ CO stretch	1,699.27	1,643	1,663	1,716	1,596	1,681	1,621[h]	1,623[i]	1,650[j]
$\nu_7(a')$ out of phase HCOH bend	1,129.49	1,092	1,122	1,135	1,079	1,129	1,107[h]	1,091[i]	
$\nu_8(a'')$ Torsion	1,042.44	978	1,034	1,072	994	1,052	993[h]		
$\nu_9(a'')CH_2$ wag	1,266.96	1,175	1,241	1,275	1,188	1,250			

[a] This work, data at the CCSD/cc-pVTZ level
[b] Ref. [23], data at the MP2/6-311(2df, 2p) level
[c] Ref. [26], data at the CCSD/aug'-cc-pVDZ level
[d] Ref. [28], data at the MP2//HF/6-31G(d,p) level
[e] Ref. [29], data at the QCISD/6-31G(d) level
[f] Ref. [29], data at the MP2/6-311+G(2d, p) level
[g] Ref. [3], vibrational frequency of the cation
[h] Ref. [23], vibrational frequency of the $\tilde{B}^2A'(3p)$ radical
[i] Ref. [34], vibrational frequency of the $\tilde{B}^2A'(3p)$ radical
[j] Ref. [33], vibrational frequency of the $\tilde{B}^2A'(3p)$ radical

Anyway, to clarify the difference between the present results and those of Johnson and Hudgens [23], we will consider the effect of the ν_9 wagging mode.

In a similar way to that of Ref. [23], we define the wagging coordinate, τ, as the variation from equilibrium of the angle between the planes H3C2H4 and XC2O1 (see Fig. 1c). We perform a conformational analysis, taking into account the inversion symmetry of the τ coordinate, considering a range of values from 0° to 40° in increments of 10° (5 points). Kinetic and potential terms are obtained by fitting a Taylor series in the τ coordinate to the a_1 representation of the G4 non-rigid group. As in the one-dimensional torsional case, the data used for the potential energy fit were corrected using the VAC. The results are collected in Table 5. We observe that the proposed expression accurately fits the data.

Due to the inversion symmetry of the τ coordinate, we use for the variational treatment basis functions symmetry adapted to the a_1 and a_2 irreducible representations of the G_4 non-rigid group. A total of 26 and 25 basis functions is used for the a_1 and a_2 representation, respectively. With this basis size, convergence in the first five energy levels is achieved. The energy levels are collected in Table 6. We observed that our one-dimensional wagging model yields a $v_9 = 0 \rightarrow 1$ frequency of 1,252.89 cm^{-1}. This value is closer than the harmonic (1,266.96 cm^{-1}) to the 1,175 cm^{-1} found with the two-dimensional model of Ref. [23]. Thus, respect to wagging, the one and two-dimensional models yield similar results.

To compare our results with those of Johnson and Hudgens [23], we build a two-dimensional model for torsion and wagging, using the θ and τ coordinates, respectively. θ and τ were varied from 0° to 90° and from −40° to 40° (90 points), respectively. Figure 4 shows the resulting potential energy hypersurface (without VAC). The potential hypersurface shows a double minimum arising from the θ coordinate rotational symmetry, see Fig. 4, for $\theta = 0°$ and 180°, with $\tau = 0°$. These minima correspond to the equilibrium structure. On the other hand, we observe a saddle point located at $\tau = 0°$. This is the same saddle point found as the maximum of energy for the torsional motion in the one-dimensional study (see Fig. 2). The kinetic terms are obtained for each (θ, τ) couple from the elements of the roto-vibrational G matrix. Now, three kinetic terms appear; B_θ, B_τ, and $B_{\theta\tau}$, corresponding to the torsion, wagging and torsion–wagging coupling. For the equilibrium conformation we find $B_\theta = 33.11$, $B_\tau = 41.84$, and $B_{\theta\tau} = 2.65\ cm^{-1}$. In similar form to the previous models, kinetic and potential energy functions are obtained by fitting to a two-dimensional Fourier + Taylor series expansions in θ and τ, respectively. The fits are symmetry-adapted to the a_1 representation of the G_4 non-rigid group, by projecting on the a_1 representation. We consider θ values in the range −60° to 60°, since it provides the best results according to the correlation coefficient, R^2, and standard deviation, σ. The data used for the potential energy fit were corrected using the VAC. Table 7 collects the resulting kinetic and potential functions. From the results collected in Table 7 we observe

Table 5 Fits of the potential and kinetic terms for protonated formaldehyde. One-dimensional models

Torsion			Wagging		
Term	V(θ)	B(θ)	Term	V(τ)	B(τ)
Cte.	3,790.1787	35.9456	Cte.	–	41.5096
cos(2θ)	−4,192.5806	−4.4897	τ^2	2.9098	–
cos(4θ)	402.4019	2.3172	τ^4	-4.2757×10^{-5}	6.6674×10^{-7}
cos(6θ)	–	−0.8983			
R^2	0.999	0.987	R^2	1.000	0.993
σ	105.830	0.276	σ	0.953	0.060

that the expansions proposed fit accurately the data, with a σ value close to the value found for the torsion. The small value of the mixed coefficients in the potential terms suggests a small but clear potential coupling between the torsion and wagging motions, see Table 7.

In the present model, the anharmonic Hamiltonian is solved by using hybrid free rotor (torsion) + harmonic oscillator (wagging) basis functions symmetry adapted to each representation of the G_4 non-rigid group. In total, 105 basis functions were used for the a_1, a_2, b_1, and b_2 representations. This basis size attains convergence in the first eight energy levels for each representation. The torsional + wagging energy levels are collected in Table 8. Now, we observe a tunnelling splitting of a few hundredths of wavenumber. The calculated frequency for the $v_8 = 0 \rightarrow 1$ torsional transition is 931.93 cm^{-1}. A value of 993 cm^{-1} was reported by Johnson and Hudgens [23], from its two-dimensional wagging + torsion study, from data obtained at the MP2/6-311+G(2df, 2p). We can attribute mainly the difference to the inclusion, through the VAC, of the average coupling with the remaining vibrations. These values are larger than the 844.12 cm^{-1} obtained from our previous one-dimensional model. On the other hand, the present calculations yield a $v_9 = 0 \rightarrow 1$ wagging frequency of 1,255.82 cm^{-1}. Johnson and Hudgens [23] found 1,175 cm^{-1} for this frequency in their two-dimensional study. The present value is slightly larger than the 1,252.89 cm^{-1} found with the one-dimensional models. These results suggest that the coupling between torsion and wagging is important in determining the torsional frequency. Thus, torsion and wagging need to be considered coupled in the vibrational models.

On the other hand, the structural variation of the α angle as a function of θ observed in Fig. 3, suggests a significant coupling of these two coordinates. Thus, we build a two-dimensional model using the θ and α coordinates. α is related to the bending vibrational mode, but cannot be considered a true bending coordinate, since bending involves also the angle H3C2H4, (see Fig. 1). To perform the two-dimensional study, α was varied in the range 90° to 180°, and θ from 0° to 90° using increments of 10° (100 points).

Table 6 Vibrational energy levels for the torsional and wagging motions of protonated formaldehyde. Energy data in cm^{-1}

Torsion[a]			Wagging[b]		
v_8	Symm.	Energy	v_9	Symm.	Energy
0	a_1, b_1	0.00	0	a_1	0.00
1	a_2, b_2	844.12	1	a_2	1,252.89
2	a_1, b_1	1,702.74	2	a_1	2,501.55

[a] First energy level at 419.93 cm^{-1} of the potential well
[b] First energy level at 627.65 cm^{-1} of the potential well

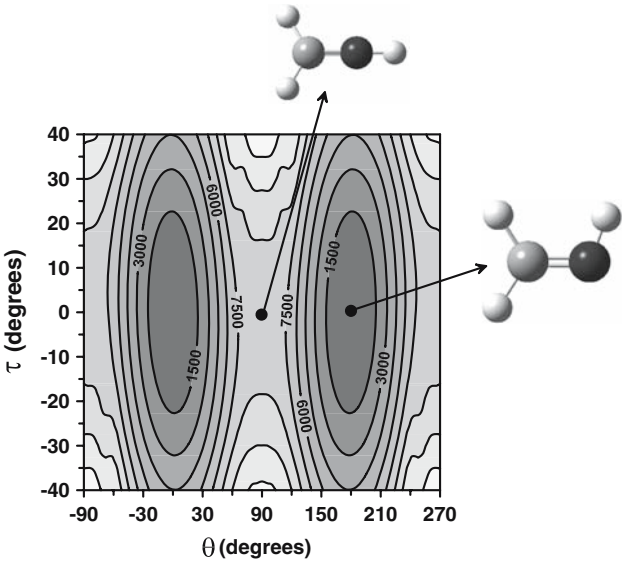

Fig. 4 Isocontour potential energy map as a function of the θ torsion angle and the wagging coordinate, τ. Interval between isocontour lines 1,500 cm^{-1}. *Darker zones* correspond to lower energy zones. The structures of the minimum and saddle point are included

Figure 5 shows the resulting potential energy hypersurface (without VAC). The potential hypersurface shows a double minimum arising from the θ coordinate rotational symmetry, (see Fig. 5), for $\theta = 0°$, $\theta = 180°$, and $\alpha = 115.12°$. On the other hand, we observe a saddle point at $\alpha = 180°$. This is

Table 7 Fits of the potential and kinetic terms for protonated formaldehyde. Two-dimensional wagging + torsion model

Wagging + torsion				
Term	$V(\theta,\tau)$	B_θ	$B_{\theta\tau}$	B_τ
Cte.	4,238.5696	38.6001	0.9939	40.4336
$\cos(2\theta)$	−4,332.7618	−8.2798	0.4496	1.1989
$\cos(4\theta)$	−154.4226	3.6873	–	–
$\cos(6\theta)$	248.6148	−1.0203	0.1546	–
τ^2	2.8568	−0.0014	−0.0006	0.0001
τ^4	-4.8982×10^{-5}	–	6.7185×10^{-07}	1.1481×10^{-06}
τ^6	–	-6.3671×10^{-11}	-3.7432×10^{-10}	-3.1444×10^{-10}
$\cos(2\theta)\tau^2$	0.1067	0.0009	−0.0003	−0.0006
$\cos(2\theta)\tau^4$	5.6295×10^{-5}	–	–	–
$\cos(2\theta)\tau^6$	–	1.9840×10^{-10}	2.2184×10^{-10}	7.9482×10^{-11}
$\cos(4\theta)\tau^2$	–	−0.0002	−0.0004	−0.0002
$\cos(4\theta)\tau^4$	–	-2.8811×10^{-07}	1.1778×10^{-06}	7.2941×10^{-07}
$\cos(4\theta)\tau^6$	1.8109×10^{-8}	–	-5.7931×10^{-10}	-2.7021×10^{-10}
$\cos(6\theta)\tau^2$	–	–	−0.0005	–
$\cos(6\theta)\tau^4$	–	1.2353×10^{-07}	2.3502×10^{-07}	-2.7461×10^{-07}
$\cos(6\theta)\tau^6$	–	–	–	1.3313×10^{-10}
$\sin(\theta)\tau$	18.0502	−0.0096	−0.0514	0.0334
$\sin(\theta)\tau^3$	−0.0023	-1.4390×10^{-05}	–	8.2972×10^{-06}
$\sin(\theta)\tau^5$	–	3.4711×10^{-09}	-6.3694×10^{-09}	-4.8502×10^{-09}
$\sin(3\theta)\tau$	4.4500	0.0114	−0.0172	−0.0067
$\sin(3\theta)\tau^3$	−0.0016	7.2499×10^{-06}	–	-2.5880×10^{-06}
$\sin(3\theta)\tau^5$	–	–	1.6453×10^{-09}	–
$\sin(5\theta)\tau$	−6.2469	–	0.0037	–
$\sin(5\theta)\tau^3$	0.0016	-4.7512×10^{-06}	–	2.7699×10^{-06}
$\sin(5\theta)\tau^5$	–	–	–	-1.3004×10^{-09}
R^2	0.999	0.998	0.991	0.998
σ	115.049	0.102	0.125	0.039

the same saddle point found as the maximum of energy for the torsional motion in the one-dimensional study (see Fig. 2). The kinetic terms are obtained at each (θ,α) couple from the elements of the roto-vibrational G matrix. Now, three kinetic terms appear; B_θ, B_α, and $B_{\theta\alpha}$, corresponding to the torsion, bending and torsion-bending coupling. For the equilibrium conformation we find $B_\theta = 33.05$, $B_\alpha = 19.81$, and $B_{\theta\alpha} = 0.0\,\mathrm{cm}^{-1}$. In this case, kinetic and potential energy functions are obtained by fitting to a two-dimensional Fourier + Taylor series expansions in θ and α, respectively. As usual, the fits are symmetry-adapted to the a_1 representation of the G_4 non-rigid group, by projecting on the a_1 representation. Due to the collinearity of the C2, O1 and H5 atoms, we select a range of 90–150° for the α angle. Table 9 collects the resulting kinetic and potential functions. The potential energy fit used data corrected with the VAC. The accuracy of the fits was assessed by the R^2 and σ estimates. From the results collected in Table 9, we observe that the expansions proposed fit the data in a similar way to the torsion and wagging + torsion models. The existence of terms with large mixed coefficients in θ and α shows an important coupling between both coordinates.

As in the previous two-dimensional model the Hamiltonian is solved using hybrid free rotor + harmonic oscillator basis functions symmetry adapted to each irreducible representation. A total of 60 basis functions was used for the a_1 representation, and 55 for the a_2, b_1, and b_2. This basis size attains convergence in the first ten energy levels for each representation. The torsional + bending energy levels are collected in Table 8. The calculated frequency for the $\nu_8 = 0 \rightarrow 1$ torsional transition is $762.32\,\mathrm{cm}^{-1}$. The pseudo-bending coordinate, α, yields a $\nu_7' = 0 \rightarrow 1$ frequency of $1{,}202.66\,\mathrm{cm}^{-1}$. However, due to the lack of correspondence of α with the actual bending coordinate this value can not be taken as

Table 8 Vibrational energy levels for the two-dimensional, wagging + torsion and bending + torsion anharmonic models of protonated formaldehyde. Energy data in cm^{-1}

Wagging + torsion[a]				Bending + torsion[b]			
ν_9	ν_8	Symm.	Energy	ν_7'[c]	ν_8	Symm.	Energy
0	0	a_1	0.00	0	0	a_1, b_1	0.00
0	0	b_2	0.01	1	0	a_1, b_1	1,202.66
0	1	a_2, b_1	931.93	0	1	a_2, b_2	762.32
1	0	a_2	1,255.82	1	1	a_2, b_2	1,969.55
1	0	b_1	1,255.86	0	2	a_1, b_1	1,594.27
0	2	a_2	1,910.58				
0	2	b_2	1,910.59				

[a] The first energy level is placed at 1083.02 cm^{-1} of the potential well
[b] The first energy level is placed at 736.22 cm^{-1} of the potential well
[c] ν_7' corresponds to the pseudo-bending mode

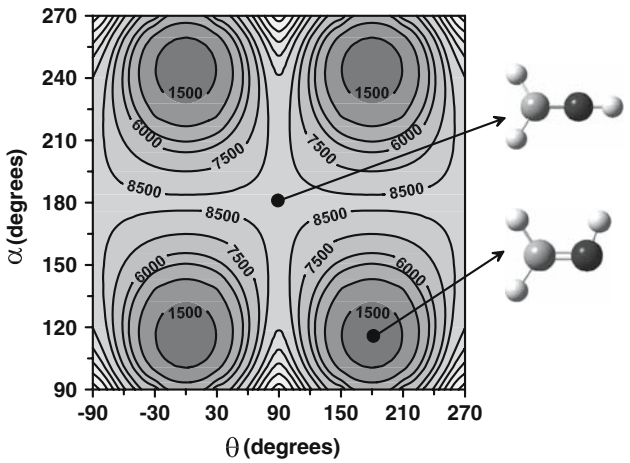

Fig. 5 Isocontour potential energy map as a function of the θ torsion and α bending angles. Interval between isocontour lines 1,500 cm^{-1}. *Darker zones* correspond to lower energy zones. The structures of the minimum and saddle point are included

estimation for the bending vibrational mode. The frequency of the torsional mode is much smaller than in the previous models. This fact shows the existence of an important coupling between torsion and bending, although the lack of correspondence between α and the ν_7 mode prevents us from giving an absolute meaning to the value.

4 Conclusions

In this work, we present a structural and vibrational study of protonated formaldehyde in its $\tilde{X}^1A'$ground electronic state at the CCSD/cc-pVTZ level of theory. The results show the equilibrium conformation to be a planar C_s symmetry structure, in agreement with the previous theoretical work. The maximum for the barrier to rotation of the H_2C moiety is found for a conformation where the COH atoms are collinear, corresponding to a first order saddle point on the potential energy hypersuface. The barrier is found 8,550.95 cm^{-1} corresponding to the rotation of the H_2C group, but also to the bending barrier for the COH angle. Considering the contribution of the remaining vibrations to torsion (i.e., the contribution to the zero point energy) the barrier becomes 8,145.19 cm^{-1}.

The dependence of the structure with the torsional motion is studied by analysing the variation of structural parameters with the torsional angle, θ. We find a clear dependence of the COH bending and the H_2C out-of-plane wagging angles with torsion. These coordinates, together with the torsion, are associated to the three vibration modes of lower frequency. This fact suggests that these three vibrational motions should be coupled together. On the other hand, the CO and OH distances reach a maximum in the interval $50° \leq \theta \leq 60°$, as a consequence of the poor orientation for conjugation of the p_z orbitals of carbon and oxygen. On the other hand, the minimum for both distances appears at the maximum of the torsion barrier, for a COH angle of 180°. This is a consequence of the collinearity of the C, O and H atoms that corresponds to the most favourable position for conjugation of the carbon and oxygen $2p_z$ orbitals.

One-dimensional anharmonic models for torsion and the H_2C wagging were built. These models are adapted to the non-rigid group symmetry of CH_2COH^+, and include the average effect of the coupling with the remaining vibrations. The corresponding vibrational Hamiltonians are variationally solved. They yield fundamental frequencies of 844.12 and 1,252.89 cm^{-1} for torsion and wagging, respectively. The frequency for wagging is not too far from the 1,175 cm^{-1} found previously by Johnson and Hudgens [23] from a two-dimensional wagging + torsion anharmonic model. However,

Table 9 Fits of the potential and kinetic terms for protonated formaldehyde. Two-dimensional bending + torsion model

Bending + torsion				
Term	$V(\theta,\alpha)$	B_θ	$B_{\theta\alpha}$	B_α
Cte.	4,024.6677	31.9657	−0.2096	19.8511
$\cos(2\theta)$	−4,865.9399	0.3192	0.0409	−0.0493
$\cos(4\theta)$	841.2722	–	0.1337	0.0163
α	−34.0849	0.2977	-2.0928×10^{-3}	0.0455
α^2	4.5674	0.0192	1.0515×10^{-5}	-2.0067×10^{-4}
α^3	−0.0463	6.3406×10^{-4}	-9.0013×10^{-7}	3.7943×10^{-7}
$\cos(2\theta)\alpha$	48.2332	–	4.0790×10^{-4}	-9.4842×10^{-3}
$\cos(4\theta)\alpha$	−12.3908	–	1.2140×10^{-3}	2.0292×10^{-3}
$\cos(2\theta)\alpha^2$	1.8006	3.3576×10^{-4}	-2.3383×10^{-5}	1.6388×10^{-4}
$\cos(4\theta)\alpha^2$	−0.3988	–	–	-5.5954×10^{-5}
$\cos(2\theta)\alpha^3$	−0.0212	–	–	-1.1490×10^{-6}
$\cos(4\theta)\alpha^3$	0.0061	–	6.5421×10^{-7}	–
R^2	0.996	0.997	0.921	1.000
σ	190.643	1.153	0.036	0.015

the torsional frequency disagrees with the 978 cm^{-1} found previously in the same two-dimensional study.

To consider the coupling between torsion and COH bending and H_2C wagging, two-dimensional anharmonic models were built. Thus, a bending + torsion anharmonic Hamiltonian is constructed and variationally solved. The model includes the average effect of the coupling with the remaining vibrations. The results yield a torsion frequency of 762.32 cm^{-1}. This result differs from our one-dimensional torsional model (844.12 cm^{-1}) and the two-dimensional results of Johnson and Hudgens [23] (978 cm^{-1}). This fact shows that the coupling of torsion with the in-plane deformation of the molecule is important. On the other hand, a wagging + torsion two-dimensional Hamiltonian is also constructed. Again, the model includes the average effect of the remaining vibrations. The Hamiltonian is solved variationally, yielding frequencies of 931.93 and 1,255.82 cm^{-1} for torsion and wagging, respectively. A small tunnelling splitting of a few hundredths of wavenumber is observed. Now, the results are close to the 978 and 1,175 cm^{-1} values found by Johnson and Hudgens [23]. The torsional frequency differs from the 844.12 cm^{-1} one-dimensional result, showing the existence of coupling between torsion and wagging.

The previous results show the existence of an important coupling among the three lowest frequency vibration modes of protonated formaldehyde: torsion, wagging and bending. However, whereas torsion and wagging can be described with a single curvilinear, internal, coordinate, the same is not true for bending, since it involves not only the COH angle, but also the HCH angle of the H_2C moiety.

Acknowledgments This work has been cofinanced by FEDER funds and the *Consejería de Educación y Ciencia de la Junta de Comunidades de Castilla-La Mancha* (grant # PBI05-009), and the *Ministerio de Educación y Ciencia* (grant # FIS2005-00293). M. E. Castro thanks the *Consejo Nacional de Ciencia y Tecnología*, *CONACyT* (Mexico) for a graduate grant (grant # 171982).

References

1. Snyder LE, Buhl D, Zuckerman B, Palmer P (1969) Phys Rev Lett 22:679–681
2. Palmer P, Zuckerman B, Buhl D, Snyder LE (1969) Astrophys J (Lett) 156:L147–L150
3. Amano T, Warner HE (1989) Astrophys J 342:L99–L101
4. Haney MA, Franklin JL (1969) Trans Faraday Soc 65:1794–1804
5. Ros P (1968) J Chem Phys 49:4902–4916
6. Haney MA, Patel JC, Hayes EF (1970) J Chem Phys 53:4105–4106
7. Schleyer PvR, Jemmis ED, Pople JA (1978) J Chem Soc Chem Commun 190–191
8. Dill JD, Fischer CL, McLafferty FW (1979) J Am Chem Soc 101(22):6532–6534
9. Nobes RH, Radom L, Rodwell WR (1980) Chem Phys Lett 74:269–272
10. DeFrees DJ, McLean AD (1985) J Chem Phys 82:333–341
11. Chomiak D, Taleb-Bendiab A, Civis S, Amano T (1994) Can J Phys 72:1078–1081
12. Ohishi M, Ishikawa SI, Amano T, Oka H, Irvine WM, Dickens JE, Ziurys LM, Apponi AJ (1996) Astrophys J 471:L61–L64
13. Purcell KF, Collins JM (1970) J Am Chem Soc 92(3):465–469
14. Ohkubo K, Yoshida T, Tomiyoshi K, Okada M (1976) J Mol Struct 34:273–281
15. Hoffmann MR, Schaefer HFIII (1981) Astrophys J 249:563–565

16. Bhattacharyya SP, Rakshit SC, Banerjee M (1983) J Mol Struct (THEOCHEM) 91:253–261
17. Dixon DA, Komornicki A, Kraemer WP (1984) J Chem Phys 81(8):3603–3611
18. DeFrees DJ, McLean AD (1986) Chem Phys Lett 131:403–408
19. Apeloig Y, Karni M (1988) J Chem Soc Perkin Trans II 625–636
20. Helgaker T, Uggerud E, Jensen HJ Aa (1990) Chem Phys Lett 173:145–150
21. Hvistendahl G, Uggerud E (1991) Organic Mass Spectrom 26:67–73
22. Stern PS, Hagler AT, Sussman F, Karpas Z (1991) J Mol Struct (THEOCHEM) 228:237–248
23. Johnson RD III, Hudgens JW (1996) J Phys Chem 100:19874–19890
24. Lee TG, Park SC, Kim MS (1996) J Chem Phys 104:4517–4529
25. Suarez D, Sordo TL (1997) J Phys Chem A 101:1561–1566
26. Del Bene JE, Gwaltney SR, Bartlett RJ (1998) J Phys Chem A 102:5124–5127
27. Jursic BS (1998) J Mol Struct (THEOCHEM) 425:193–199
28. Rhee YM, Kim MS (1998) J Chem Phys 109(13):5363–5371
29. Blowers P, Masel RI (2000) J Phys Chem A 104:34–44
30. Oiestad AML, Uggerud E (2000) Int J Mass Spectrom 201:179–185
31. Jalbout AF (2002) J Mol Struct (THEOCHEM) 594:129–133
32. Antol I, Eckert-Maksic M, Müller T, Dallos M, Lischka H (2003) Chem Phys Lett 374:587–593
33. Dyke JM, Ellis AR, Jonathan N, Deddar N, Morris A (1984) Chem Phys Lett 111(3):207–210
34. Dulcey CS, Hudgens JW (1986) J Chem Phys 84(10):5262–5270
35. Marston CC, Balint-Kurti GG (1989) J Chem Phys 91:3571–3576
36. Knowles PJ, Hampel C, Werner H-J (1991) J Chem Phys 99:5219
37. Dunning THJr (1989) J Chem Phys 90(2):1007–1023
38. Frisch MJ, Trucks GW, Schlegel HB, Scuseria GE, Robb MA, Cheeseman JR, Montgomery JA Jr, Vreven T, Kudin KN, Burant JC, Millam JM, Iyengar SS, Tomasi J, Barone V, Mennucci B, Cossi M, Scalmani G, Rega N, Petersson GA, Nakatsuji H, Hada M, Ehara M, Toyota K, Fukuda R, Hasegawa J, Ishida M, Nakajima T, Honda Y, Kitao O, Nakai H, Klene M, Li X, Knox JE, Hratchian HP, oss JB, Adamo C, Jaramillo J, Gomperts R, Stratmann RE, Yazyev O, Austin AJ, Cammi R, Pomelli C, Ochterski JW, Ayala PY, Morokuma K, Voth GA, Salvador P, Dannenberg JJ, Zakrzewski VG, Dapprich S, Daniels AD, Strain MC, Farkas O, Malick DK, Rabuck D, Raghavachari K, Foresman JB, Ortiz JV, Cui Q, Baboul AG, Clifford S, Cioslowski JA, Stefanov BB, Liu G, Liashenko A, Piskorz P, Komaromi I, Martin RL, Fox DJ, Keith T, Al-Laham MA, Peng CY, Nanayakkara A, Challacombe M, Gill PMW, Johnson B, Chen W, Wong MW, Gonzalez C, Pople JA (2003) Gaussian 03 Revision A.1 Gaussian Inc Pittsburgh PA
39. Muñoz-Caro C, Niño A (1994) Computers Chem 18(4):413–417
40. Pickett HM (1972) J Chem Phys 56:1715–1723
41. Harthcock MA, Laane J (1985) J Chem Phys 89:4231–4240
42. Niño A, Muñoz-Caro C (1994) Computers Chem 18(1):27–32
43. Muñoz-Caro C, Niño A, Moule DC (1994) Chem Phys 186:221–231
44. Niño A, Muñoz-Caro C, Moule DC (1995) J Phys Chem 99:8510–8515
45. Niño A, Muñoz-Caro C (1995) Computers Chem 19(4):371–378
46. LAVCA: General large amplitude vibrational energy levels computation program by Muñoz-Caro C and Niño A
47. Tennyson J (2000) Chapter 9. Variational calculations of rotation-vibration spectra. In Computational Molecular Spectroscopy Ed. Jensen P and Bunker PR John Wiley & Sons
48. Niño A, Muñoz-Caro C, Moule DC (1994) J Phys Chem 98(6): 1519–1524
49. Niño A, Muñoz-Caro C, Moule DC (1994) J Mol Struct (THEOCHEM) 318:237–242
50. Muñoz-Caro C, Niño A, Moule DC (1995) J Chem Soc Faraday Trans 91(3):399–403